Published in final edited form as:
Free Radic Biol Med. 2008 November 1; 45(9): 1340–1351. doi:10.1016/j.freeradbiomed.2008.08.013.

Distinct Roles of Nox1 and Nox4 in Basal and Angiotensin II-Stimulated Superoxide and Hydrogen Peroxide Production

Sergey I. Dikalov[1,*], **Anna E. Dikalova**[1], **Alfiya T. Bikineyeva**[1], **Harald H.H.W. Schmidt**[2], **David G. Harrison**[1], and **Kathy K. Griendling**[1]

1*Division of Cardiology, Department of Medicine, Emory University School of Medicine, Atlanta, GA*

2*Department of Pharmacology & Centre for Vascular Health, Monash University, Melbourne, Australia.*

Abstract

NADPH oxidases are major sources of superoxide ($O_2^{\cdot-}$) and hydrogen peroxide (H_2O_2) in vascular cells. Production of these reactive oxygen species (ROS) is essential for cell proliferation and differentiation, while ROS overproduction has been implicated in hypertension and atherosclerosis. It is known that the heme-containing catalytic subunits Nox1 and Nox4 are responsible for oxygen reduction in vascular smooth muscle cells from large arteries. However, the exact mechanism of ROS production by NADPH oxidases is not completely understood. We hypothesized that Nox1 and Nox4 play distinct roles in basal and angiotensin II (AngII)-stimulated production of $O_2^{\cdot-}$ and H_2O_2. Nox1 and Nox4 expression in rat aortic smooth muscle cells (RASMCs) was selectively reduced by treatment with siNox4 or antisense Nox1 adenovirus. Production of $O_2^{\cdot-}$ and H_2O_2 in intact RASMCs was analyzed by dihydroethidium and Amplex Red assay. Activity of NADPH oxidases was measured by NADPH-dependent $O_2^{\cdot-}$ and H_2O_2 production using electron spin resonance (ESR) and 1-hydroxy-3-carboxy-pyrrolidine (CPH) in the membrane fraction in the absence of cytosolic superoxide dismutase. It was found that production of $O_2^{\cdot-}$ by quiescent RASMC NADPH oxidases was five times less than H_2O_2 production. Stimulation of cells with AngII led to a 2-fold increase of $O_2^{\cdot-}$ production by NADPH oxidases, with a small 15 to 30% increase in H_2O_2 formation. Depletion of Nox4 in RASMC led to diminished basal H_2O_2 production, but did not affect $O_2^{\cdot-}$ or H_2O_2 production stimulated by AngII. In contrast, depletion of Nox1 in RASMC inhibited production of $O_2^{\cdot-}$ and AngII-stimulated H_2O_2 in the membrane fraction and intact cells. Our data suggest that Nox4 produces mainly H_2O_2, while Nox1 generates mostly $O_2^{\cdot-}$ that is later converted to H_2O_2. Therefore, Nox4 is responsible for basal H_2O_2 production, while $O_2^{\cdot-}$ production in non-stimulated and AngII-stimulated cells depends on Nox1. The difference in the products generated by Nox1 and Nox4 may help to explain the distinct roles of these NADPH oxidases in cell signaling. These findings also provide important insight into the origin of H_2O_2 in vascular cells, and may partially account for the limited pharmacological effect of antioxidant treatments with $O_2^{\cdot-}$ scavengers that do not affect H_2O_2.

INTRODUCTION

During the past decade, it has become apparent that production of superoxide ($O_2^{\cdot-}$) and hydrogen peroxide (H_2O_2) by NADPH oxidases plays a critical role in the genesis of many

*To whom correspondence should be addressed: Sergey Dikalov, Ph.D., FRIMCORE Director, Division of Cardiology, Emory University School of Medicine, 1639 Pierce Drive, Atlanta, GA 30322, Tel.: 404-712-9550, Fax: 404-727-4080, E-mail: dikalov@emory.edu.

vascular diseases [1,2]. Both of these reactive oxygen species (ROS) serve as second messengers to activate multiple intracellular signaling pathways [2,3]. Superoxide is one of the most the important ROS, not only because it rapidly inactivates nitric oxide [4], but also because it produces many other types of ROS, such as hydrogen peroxide (H_2O_2) and peroxynitrite ($ONOO^-$), and stimulates free radical production by releasing ferric ions from $(FeS)_4$ clusters of proteins such as aconitase [5]. However, a growing body of evidence supports an important role for H_2O_2 in cellular redox regulation which may be distinct from the effects of $O_2^{\cdot-}$ [3,6,7]. Hydrogen peroxide is involved in two-electron signaling mediated by thiols, while $O_2^{\cdot-}$ modulates one-electron redox signaling mediated by iron ions [8]. Hydrogen peroxide can be produced directly without intermediate $O_2^{\cdot-}$ by various cellular enzymes such as xanthine and glucose oxidases [9]. However, the direct H_2O_2 generation by NADPH oxidases in normal and pathological conditions remains controversial.

The NADPH oxidases are membrane-associated enzymes that catalyze 1-electron reduction of oxygen using NADPH as an electron donor. The phagocytic oxidase consists of 4 major subunits: a plasma membrane spanning cytochrome b558 composed of a large subunit gp91phox and the smaller p22phox subunit, and 2 cytosolic components p47phox and p67phox [2]. The low molecular weight G protein Rac1 participates in assembly of the active complex [2]. Vascular NADPH oxidases are structurally distinct fromthe classic phagocytic NADPH oxidase. In large arteries, smooth muscle cells lack gp91phox, the catalytic subunit that transfers electrons from NADPH to molecular oxygen to form $O_2^{\cdot-}$ [10]. Instead, these cells express the gp91phox homologues, Nox1 and Nox4 [10,11], the latter of which is also expressed in endothelial cells [12]. These two enzymes are differentially regulated by growth factors [10] and during the development and resolution of restenosis [13]. Furthermore, Nox1 and Nox4 are found in distinct intracellular compartments, suggesting that they serve different functions within the cell [14]. Indeed, Nox1 appears to mediate growth of vascular smooth muscle cells (VSMC) [15], while Nox4 is involved in VSMC differentiation [16]. Taken together, these observations suggest that ROS can affect physiological functions localized in particular compartments of the cell.

In vascular smooth muscle cells, activation of the angiotensin AT_1 receptor leads to phosphorylation of $p47^{phox}$ [17] and Src-mediated Rac1 translocation to the membrane which result in Nox1 activation in aortic VSMC [18]. Thus, acute stimulation of smooth muscle cells with Ang II increases primarily Nox1, but not Nox4 activity [10]. In contrast, Nox4 is activated by transforming growth factor-β (TGF-β) [19], but does not require $p47^{phox}$ or Rac1 subunits [11] for activation.

Upregulation of NADPH oxidase subunits and increased $O_2^{\cdot-}$ production by vascular NADPH oxidases is common in cardiovascular disease. NADPH oxidases are activated by mechanical forces, hormones and cytokines (reviewed in [3,20]). In particular, the octapeptide angiotensin II (Ang II) is an important activating stimulus for vascular NADPH oxidases. Ang II is the major effector hormone of the renin–angiotensin system and has effects in heart, vasculature and kidney [21]. ROS produced following Ang II-mediated stimulation of NADPH oxidases signal through pathways such as mitogen-activated protein kinases, tyrosine kinases and transcription factors, and lead to events such as inflammation, hypertrophy, remodeling and angiogenesis [22]. We have recently reported that vascular NADPH oxidases may serve a role of a “master oxidase”, which turns on the production of intracellular ROS by xanthine oxidase, mitochondria and uncoupled eNOS [23]. Interestingly, NADPH oxidase itself can be stimulated in a feed-forward fashion [24].

Previously, it has been shown that the phagocytic NADPH oxidase produces primarily $O_2^{\cdot-}$ [25], which then can be transformed into H_2O_2 by spontaneous or SOD-catalyzed reactions. However, the molecular structure of the vascular NADPH oxidases is very different from

phagocytic NADPH oxidase. The exact mechanism of ROS production by Nox1 and Nox4 is unclear. It is unknown whether these NADPH oxidases generate only $O_2^{\cdot-}$ or whether they can directly produce H_2O_2. This is an important distinction, because the precise biological roles of specific Nox proteins may depend on whether they generate $O_2^{\cdot-}$ or H_2O_2.

In this work we studied the production of $O_2^{\cdot-}$ and H_2O_2 by vascular NADPH oxidases in rat aortic smooth muscle cells (RASMCs). Depletion of Nox4 in RASMC led to diminished basal production of H_2O_2, but did not affect $O_2^{\cdot-}$ generation. In contrast, depletion of Nox1 inhibited production of $O_2^{\cdot-}$ and AngII-stimulated H_2O_2 in intact cells and the membrane fraction. Our data suggest that Nox4 produces mainly H_2O_2, while Nox1 generates mostly $O_2^{\cdot-}$ that is later converted to H_2O_2.

Methods

Reagents

Cyclic hydroxylamine 1-hydroxy-3-carboxy-pyrrolidine (CPH) and nitroxide 3-carboxy-proxyl (CP) were purchased from Alexis Corporation (San Diego, CA). Diethylenetriaminepentaacetic acid (DTPA), superoxide dismutase from bovine erythrocyte (SOD), xanthine and cytochrome c were obtained from Sigma (St. Louis, MO). Xanthine oxidase was purchased from Roche Molecular Biochemicals (Indianapolis, IN). All other reagents were obtained from Sigma (St Louis, MO). Amplex Red was purchased from Invitrogen Corporation (Carlsbad, CA). Rabbit polyclonal antibody anti-Nox4 was a kind gift from Dr. David Lambeth (Emory University). CPH was dissolved in oxygen-free (bubbled for 20 minutes with argon) 0.9% NaCl with 1 mM DTPA. A stock solution of CPH (10mM) was kept on ice and prepared daily.

Cell culture

Rat aortic smooth muscle cells (RASMCs) were isolated from rat aortas by enzymatic digestion as previously described [26]. Cells were grown in Dulbecco's modified Eagle's medium (DMEM) containing 4.5 g/l glucose, 2 mM glutamine, 100 U/ml penicillin, and 100 μg/ml streptomycin and supplemented with 10% calf serum. RASMCs were made quiescent by incubation in culture medium with 0.1% serum for 2-days, and stimulated with 100 nM Ang II for 4 hours where indicated.

Small interference RNA (siRNA) nox4 silencing experiments

For assessment of the role of Nox4 in ROS production, RASMCs (30–40% confluence) were treated with siRNA for 4–6 days prior to ROS analysis, as we have described previously [27]. The annealed siRNA duplexes for nox4 (sense: 5'-ACUGAGGUACAGCUGGAUGUU-3', antisense:5'-CAUCCAGCUGUACCUCAGUUU-3'), and for non-silencing siRNA were purchased from Ambion. RASMCs were transfected with a final siRNA duplex at a concentration of 15 to 30 nM using Oligofectamine (Invitrogen, Carlsbad, CA, USA) in OPTI-MEM. After 6 hrs, the medium was replaced with DMEM plus 10% fetal bovine serum. Following transfection, the cells were treated with Ang II to study regulation of ROS production.

Preparation of recombinant adenoviruses and infection of RASMCs

Antisense Nox1 adenovirus (AdASNox1) was prepared as described previously [10]. RASMCs were infected for 2 hours with recombinant adenovirus in serum free culture medium, and incubated for another 4 days in the same medium without virus before harvesting for protein extraction.

Preparation of membrane fractions from cultured rat aortic smooth muscle cells (RASMCs)

Membrane samples from RASMCs were prepared as described previously [28,29]. Briefly, cells were harvested, washed twice with ice-cold PBS, scraped, centrifuged at 400 × *g* (10 min), and resuspended in 1 ml of lysis buffer (50 mM phosphate (treated for 2 h with 5 g/100 ml Chelex-100 and filtered) containing the protease inhibitors aprotinin (10 μg/ml), leupeptin (0.5 μg/ml), pepstatin (0.7 μg/ml), and PMSF (0.5 mM) (pH 7.4)). Cells were sonicated (power 3 W, using Microson 2425 from Misonix, Inc.) for 10 s on ice and centrifuged at 28,000 × *g* for 15 min at 4°C. The membrane pellet was resuspended in 150 μl of lysis buffer and protein concentration was measured using the Bradford method.

It is important to note that membrane fractions isolated by this protocol have been extensively used for measurements of NADPH oxidase activity [28–31]. Neither NO synthases, mitochondria nor xanthine oxidase contribute to NADPH-stimulated ROS production in these membrane fraction, while depletion of NADPH oxidases or treatment of tissue with the NADPH oxidase inhibitor apocynin significantly decreased NADPH-stimulated ROS production in these fractions [28–32].

Electron Spin Resonance (ESR)

ESR was used to measure $O_2^{\cdot-}$ and H_2O_2 production in membrane fractions. ESR methods were validated in the xanthine oxidase system (Figure 1) which generates both $O_2^{\cdot-}$ and H_2O_2 [33]. It contained xanthine oxidase (2 U/ml), xanthine (0.1 mM), and DTPA (0.2 mM) in 50 mM sodium phosphate buffer saline (PBS, pH 7.4). Detection of superoxide radical was confirmed by inhibition of the ESR signal by superoxide dismutase (50 U/ml). Superoxide production in cell homogenate or membrane fraction was measured in samples containing 10 μg protein, 1 mM CPH, 100 μM NADPH and 0.1 mM DTPA in a total volume of 100 μl of Chelex-treated PBS.

Production of H_2O_2 was measured by co-oxidation of CPH in HRP-acetamidophenol (AAP) reaction. Each molecule of H_2O_2 forms 2 molecules of CP by two consecutive peroxidase reactions of compound I and compound II. Detection of H_2O_2 was confirmed by inhibition with 50 μg/ml catalase (Figure 1).

To measure production of H_2O_2 by NADPH oxidases [28] in membrane preparations of RASMC, ten μg protein was incubated with 50 U/ml SOD, 1 U/ml horseradish peroxidase (HRP), 1 mM AAP, 100 μM NADPH, 0.2 mM DTPA, and 1 mM CPH in a total volume of 100 μl of Chelex-treated PBS. Catalase-inhibited CP-formation in the sample with HRP and AAP was equal to the amount of H_2O_2 [34]. Quantitative measurement of $O_2^{\cdot-}$ and H_2O_2 was confirmed by analysis of ROS production by xanthine and xanthine oxidase in the presence of membrane fractions.

In order to test the effect of inhibition of Cu,Zn-SOD on superoxide detection, membrane fractions and cell homogenates (2 mg/ml) were incubated for 15 minutes with 1 mM diethyldithiocarbamate (DETC) and then samples were diluted to 0.1mg/ml protein for ESR measurement. This method has been widely used in intact cells, tissue and homogenates in order to inhibit Cu,Zn-SOD by removing Cu from SOD [35]. In experiments with intact RASMC, cells were incubated for 30-minutes with 1 mM DETC and then washed before superoxide detection.

Measurements of xanthine oxidase activity

Activity of xanthine oxidase was determined by measuring oxidation of 50 μM xanthine to uric acid (295 nm, 11,000 M^{-1} cm^{-1}) and following the SOD-inhibited reduction of 50 μM

cytochrome c (550 nm, 21,000 M^{-1} cm^{-1}) using a Shimadzu UV2401PC spectrophotometer (Columbia, MD).

ESR settings

All ESR measurements were performed by EMX ESR spectrometer (Bruker) equipped with a super-high Q microwave cavity. The ESR instrument settings for experiments with membrane fractions were as follows: field sweep, 50 G; microwave frequency, 9.78 GHz; microwave power, 20 mW; modulation amplitude, 2 G; conversion time, 656 ms; time constant, 656 ms; 512 points resolution and receiver gain, 1×10^5. Kinetics were recorded using 1312 ms conversion time, 5248 ms time constant, and monitoring the ESR amplitude of low-field component of ESR spectrum of CP nitroxide.

High-performance liquid chromatography (HPLC)

Superoxide production in intact cells was measured by dihydroethidium (DHE) with an HPLC-based assay [36]. Briefly, cells were washed with Krebs/HEPES buffer and incubated with 10 μM DHE for 20 min at 37°C. Media was removed and cells were transferred to methanol for extraction of the superoxide-specific product hydroxyethidium and kept at −20°C. Separation of ethidium, hydroxyethidium and dihydroethidium was performed using a Beckman HPLC System Gold model with a C-18 reverse phase column (Nucleosil 250, 4.5 mm; Sigma-Aldrich), equipped with both UV and fluorescence detectors. Fluorescence detection at 580 nm (emission)/480 nm (excitation) was used to measure 2-hydroxyethidium.

Amplex Red assay

H_2O_2 measurements in intact cells were made using the horseradish peroxidase-linked Amplex Red fluorescence assay as previously described [37]. Briefly, Amplex Red (50 μM) and horseradish peroxidase type II (0.1 U/ml) were added to the cellular samples. Fluorescence readings were made in triplicate in a 96-well plate at Ex/Em = 530/580 nm using 100-μl samples of media. H_2O_2 concentration was calculated using a standard curve and normalized to cellular protein as measured by the Bradford assay.

Quantitative real-time polymerase chain reaction

Total RNA was isolated from cells using the RNeasy kit, as recommended by the manufacturer. Quantitation of Nox1, Nox4 and 18S rRNA, was performed by amplification of RASMC cDNA using the LightCycler (Roche) real-time thermocycler with gene-specific primers [38]. Copy number was calculated by the instrument software from standard curves of genuine templates.

Immunoblotting

RASMCs were lysed in the presence of 1% Triton X-100 as described previously [14], and lysates were divided into Triton-soluble and insoluble fractions by centrifugation. Proteins were separated using SDS-PAGE and transferred to nitrocellulose membranes, blocked, and incubated with primary antibodies. Proteins were detected by ECL. Band intensity was quantified by densitometry of immunoblots using Image J. Rabbit polyclonal antibodies anti-Nox4 and anti-Nox1 (1:1000 dilution) were used as characterized previously [14,39]. Nox1 antibodies were provided by Dr. Harald H.H.W. Schmidt.

Statistics

Experiments with NOX1 and NOX4 depletion were analyzed using analysis of variance (ANOVA). Post hoc analysis to detect differences between specific groups was accomplished with the Student Neuman Keuls test. In all other experiments, data were analyzed with

Student's t-test to determine the significance of treatment effects. The level of statistical significance was taken as $p < 0.05$.

RESULTS

Validation of ESR measurements of $O_2^{\cdot-}$ and H_2O_2 using the xanthine oxidase system

It is known that xanthine oxidase generates both $O_2^{\cdot-}$ and H_2O_2 simultaneously. Furthermore, production of H_2O_2 exceeds generation of $O_2^{\cdot-}$ [9]. Therefore, we validated our new ESR assay for measurement of $O_2^{\cdot-}$ and H_2O_2 using the xanthine oxidase system.

We previously reported that the reaction of hydroxylamine probe CPH with $O_2^{\cdot-}$ produces 3-carboxy-proxyl (CP), which is inhibited by superoxide dismutase (SOD) [40]. Indeed, addition of xanthine and xanthine oxidase to CPH led to a steady rise in ESR amplitude of nitroxide radical, which was completely blocked by SOD supplementation (Figure 1A). It is important to note that separate addition of xanthine or xanthine oxidase did not change background oxidation of CPH (Figure 1A). Increasing the CPH concentration did not affect the amount of SOD-inhibitable nitroxide formation. These data confirm that $O_2^{\cdot-}$ formation can be quantitatively measured using CPH in the absence of cellular antioxidants.

Previously, it has been described that peroxidase activity can be measured by peroxidase/acetamidophenol-mediated co-oxidation of cyclic hydroxylamines to nitroxide [41]. We have adapted this technique to measure the production of H_2O_2 (Figure 1B). This new ESR technique allowed us to quantify the formation of H_2O_2 by co-oxidation of CPH in the horseradish peroxidase/acetamidophenol reaction, where one molecule of H_2O_2 will produce two CP-radicals. It was found that addition of horseradish peroxidase (HRP) or acetamidophenol (AAP) did not significantly change the background oxidation of CPH (Figure 1B). Addition of xanthine and xanthine oxidase to the probe containing HRP, AAP and CPH led to strong accumulation of 3-carboxy-proxyl, which was not inhibited by SOD, but was completely blocked by catalase (Figure 1B). These data confirm that the production of H_2O_2 can be measured by HRP/acetamidophenol-mediated co-oxidation of CPH in the absence of cellular H_2O_2 scavengers. It is important to note that an increase in the concentrations of CPH, AAP or HRP did not affect accumulation of the catalase-inhibited nitroxide.

Of importance, H_2O_2 was measured in the presence of SOD (50 U/ml) in order to avoid the complication of superoxide reacting with CPH. Therefore, the yield of total H_2O_2 was not altered. We further validated these independent ESR protocols for detection of superoxide or H_2O_2 to ensure artifact free and quantitative detection of these species by comparing the rate of xanthine oxidation with ROS measurements by ESR. Oxidation of xanthine by xanthine oxidase was measured by urate accumulation (740 nM/min), and was almost identical to accumulation of total H_2O_2 (721 nM/min) measured by ESR in the presence of SOD, HRP, acetamidophenol and CPH. In this assay, oxidation of CPH was completely inhibited by catalase (10 μg/ml). Production of superoxide by xanthine oxidase measured by cytochrome c reduction (530 nM/min) was identical to superoxide detection by CPH (541 nM/min). Both cytochrome C reduction and CPH oxidation in the superoxide assay was inhibited by Cu,Zn-SOD (50 U/ml). These data confirm specific and quantitative detection of superoxide and H_2O_2 by these ESR methods in the absence of cellular antioxidants.

In order to compare $O_2^{\cdot-}$ production (530 nM/min) to total xanthine oxidase activity (740 nM/min), urate accumulation should be multiplied by factor of 2 because the formation of urate releases two electrons, while cytocrome c receives only one electron from superoxide. Therefore, the yield of superoxide formation by xanthine oxidase determined spectrophotometrically is 530/1480, or 36%. ESR measurements provide similar results (541/1442 or 37%). This means that 1/3 of electrons produced superoxide, while 2/3 of electron

flow generated H_2O_2 by 2-electron reduction of oxygen. These estimates are in line with the previously reported ratio of one- and two-electron oxygen reduction by xanthine oxidase [9, 33].

Analysis of NADPH oxidase activity by NADPH-dependent $O_2^{\cdot-}$ and H_2O_2 production in the membrane fraction

After validation using the xanthine oxidase system, we used this assay to analyze NADPH oxidase activity in the membrane fraction of RASMCs, measuring both $O_2^{\cdot-}$ and H_2O_2 (Figure 2A). Accumulation of 3-carboxyproxyl (CP) was followed by an increase in intensity of the low-field component of ESR spectrum (Figure 2A, insert). Addition of NADPH to CPH and the membrane fraction strongly increased the ESR signal, which was inhibited by SOD. Thus, production of $O_2^{\cdot-}$ by NADPH oxidases can be measured as NADPH-dependent formation of CP nitroxide, which is also inhibited by SOD (Figure 2A).

Addition of NADPH to the membrane fraction in the presence of SOD, HRP and acetamidophenol gave rise to an ESR signal that was inhibited by catalase (Figure 2A). It is important to note that NADPH failed to stimulate nitroxide formation in the absence of the membrane fraction. An increase in the concentrations of HRP and AAP did not affect the detection of H_2O_2 in membrane fractions, which confirms quantitative H_2O_2 measurements (data not shown).

It is conceivable that the reaction of $O_2^{\cdot-}$ with some cellular components (Cu,Zn-SOD, iron-sulfur clusters, ascorbate) at rate constants orders of magnitude greater than that with CPH could underestimate $O_2^{\cdot-}$ production in the membrane fractions. This should not be an issue with these measurements, however, because membrane fractions do not contain cytoslic Cu,Zn-SOD, GSH or ascorbate. Nevertheless, we studied possible interference with superoxide detection by CPH by comparing detection at different concentrations of CPH (rate constant $3.2\times10^3\ M^{-1}s^{-1}$), and comparing CPH with CMH (rate constant $1.2\times10^4\ M^{-1}s^{-1}$) and dihydroethidium (rate constant $2\times10^6\ M^{-1}s^{-1}$) [36,42]. First, increasing the CPH concentration 5-fold increased $O_2^{\cdot-}$ detection by less than 10% (Fig.2B, C). Second, application of the CMH probe, which has a 4-times higher rate constant with $O_2^{\cdot-}$ [36], did not affect $O_2^{\cdot-}$ detection (Figure 2B). Third, application of the SOD inhibitor DETC did not increase detected $O_2^{\cdot-}$ (data not shown). Fourth, in the membrane fraction of AngII-stimulated RASMCs, DHE/HPLC and CPH detected approximately the same amount of superoxide (456 and 410 pmol/mg/min). Taken together, these experiments suggest that 1 mM CPH detects approximately 90% of the superoxide in the membrane fraction in the absence of a competing target for the superoxide, such as superoxide dismutase.

In contrast, superoxide detection was not quantitative in the cell homogenate, which is likely due to the presence of cytosolic Cu,Zn-SOD (Figure 2C, D). Indeed, supplementation with the SOD inhibitor DETC significantly increased $O_2^{\cdot-}$ detection in the cell homogenate (Figure 2D), but not in the membrane fraction (data not shown). CMH was much more effective than CPH for $O_2^{\cdot-}$ detection in the cell homogenate (Figure 2D). Furthermore, $O_2^{\cdot-}$ detection was dependent upon CPH concentration in the cell homogenate, but not in the membrane fraction (Figure 2C), which is likely due to competition of CPH with antioxidants for $O_2^{\cdot-}$ in the homogenate, but not in the membrane fraction.

It is important to note that the presence of reducing agents such as NADPH, xanthine or GSH is can create problems for H_2O_2 detection. For example, horseradish peroxidase oxidation of Amplex Red failed to measure H_2O_2 production by xanthine oxidase in the membrane fraction due to the reduction of Amplex Red radical by NADPH or xanthine [43]. Addition of Amplex Red to the xanthine oxidase system after oxidation of xanthine detected only 31% of H_2O_2 when compared to urate accumulation and ESR method. However, in our system H_2O_2

detection was not affected by the presence of NADPH (25–500 μM) or xanthine (25–500 μM), which is likely due to the rapid reaction of CPH with acetamidophenyl radical.

As we described in the previous section, measurements of H_2O_2 represent the sum of dismutated $O_2^{\cdot-}$ and $O_2^{\cdot-}$ -independent H_2O_2 production. Interestingly, detection of NADPH-dependent ROS (Figure 2A) showed that production of total H_2O_2 (658 pmol/mg/min) significantly exceeded the rate of $O_2^{\cdot-}$ production (184 pmol/mg/min), which suggests that $O_2^{\cdot-}$-independent H_2O_2 production was 474 pmol/mg/min. In the next sections, we investigated the role of Nox1 and Nox4 in basal and angiotensin II-stimulated $O_2^{\cdot-}$ and H_2O_2 production.

Stimulation of NADPH oxidase activity in RASMC treated with angiotensin II

The effect of angiotensin II on $O_2^{\cdot-}$ and H_2O_2 production by NADPH oxidases was tested in membrane fractions isolated from AngII-stimulated quiescent and proliferating RASMC. NADPH-dependent $O_2^{\cdot-}$ and H_2O_2 production was higher in proliferating cells compared to quiescent RASMCs (Figure 3). Stimulation of cells with AngII led to a two-fold increase in $O_2^{\cdot-}$ production both in quiescent and proliferating RASMCs (Figure 3A). However, AngII stimulation had only a minor, but significant, effect on the total H_2O_2 production. Interestingly, AngII almost doubled the ratio of $O_2^{\cdot-}$ to H_2O_2 production from 22% to 38% in quiescent cells. Proliferating RASMCs had a higher basal production of $O_2^{\cdot-}$ and H_2O_2 than quiescent cells, but AngII further increased $O_2^{\cdot-}$ production, raising the ratio of $O_2^{\cdot-}$ to H_2O_2 production from 25% to 41%. Interestingly, the amount of AngII-stimulated $O_2^{\cdot-}$ production was close to the amount of AngII-induced H_2O_2 formation (Figure 3A,B; 6B,C). Therefore, it is likely that AngII-induced H_2O_2 is mainly produced by dismutation of AngII-stimulated $O_2^{\cdot-}$. Thus, stimulation of RASMCs with AngII primarily increases $O_2^{\cdot-}$ production.

It has been previously shown that AngII stimulates Nox1 activity by PKC-dependent phosphorylation of $p47^{phox}$ [17] and Rac1 activation [18]. In this work, we investigated if a 4-hour stimulation with AngII increased $O_2^{\cdot-}$ production by altering Nox1 or Nox4 mRNA and protein levels [10,38]. Real-time PCR analysis revealed that AngII significantly increased Nox1 mRNA in both quiescent and proliferating RASMC (Figure 4A). In contrast, AngII treatment caused a minor decrease in Nox4 mRNA (Figure 4B). However, Western Blot analysis of Nox1 and Nox4 protein did not show any effect of Ang II over this time course (Figure 4C, D), although basal levels in quiescent and proliferating cells were quite different. These observations show that $O_2^{\cdot-}$ production stimulated by a 4-hour treatment with Ang II is not due to an increase in Nox1 or Nox4 protein levels, but is likely due to the previously shown PKC-dependent regulation of Nox activity.

In agreement with our previous observations [38], $O_2^{\cdot-}$ production correlates with the higher Nox1 level in proliferating RASMC (Figure 3A, 4C). Furthermore, the high Nox4 level in quiescent RASMCs correlates with the higher H_2O_2 to $O_2^{\cdot-}$ ratio in the absence AngII (Figure 3B, 4D). These data raise the possibility that Nox4 is responsible for the bulk of H_2O_2 production, while Nox1 may produce predominantly $O_2^{\cdot-}$.

Analysis $O_2^{\cdot-}$ and H_2O_2 production in Nox4-depleted RASMCs

In order to test this hypothesis, we inhibited Nox4 expression using small interference RNA [16]. Treatment of RASMCs with Nox4 siRNA resulted in a substantial decrease in Nox4 expression measured by real-time PCR and Western Blot analysis (Figure 5A, B) compared to treatment with scrambled siRNA. As noted above, stimulation of RASMCs with Ang II did not affect the Nox4 level. Furthermore, siNox4 did not significantly change the expression of Nox1 (data not shown).

To determine whether depletion of Nox4 decreases the production of cellular $O_2^{\cdot-}$, we measured intracellular $O_2^{\cdot-}$ using DHE-HPLC [44,45]. As shown in Figure 6A, basal $O_2^{\cdot-}$ production was not affected in Nox4-depleted cells (Figure 6A). Furthermore, there was no difference between AngII-stimulated generation of $O_2^{\cdot-}$ in cells treated with scrambled RNA and Nox4-depleted RASMCs (Figure 6A). Similar results were obtained using the hydroxylamine probe CMH and ESR (data not shown) [38,44]. These results suggest that Nox4 is not the main source of $O_2^{\cdot-}$, and further supports the notion that $O_2^{\cdot-}$ is mostly produced by Nox1, but not Nox4.

To investigate the effect of siNox4 on the production of cellular H_2O_2, we used the fluorescent probe Amplex Red [44]. As noted above, Amplex Red cannot measure H_2O_2 production in the membrane fraction due to reduction by NADPH or xanthine. In order to avoid this interference, we used Amplex Red to detect extracellular H_2O_2 released from intact cells. The Amplex Red signal was completely inhibited by catalase (10 μ/ml), while supplementation with Cu,Zn-SOD (50 U/ml) did not significantly affect H_2O_2 detection.

The production of cellular H_2O_2 in Nox4-depleted RASMCs was significantly lower than in cells treated with scrambled siRNA (Figure 6B). Interestingly, Nox4 depletion also reduced production of H_2O_2 in AngII-stimulated cells (Figure 6B, sinox4+AngII); however, when compared to the corresponding baseline, the AngII-stimulated increase in cellular H_2O_2 was 71% in scrambled siRNA treated cells and 67% in siNox4 treated cells. This agrees well with the values of the AngII-induced increase of $O_2^{\cdot-}$ production, suggesting that H_2O_2 produced in response to AngII is the product of $O_2^{\cdot-}$ dismutation.

Measurements of $O_2^{\cdot-}$ and H_2O_2 production in intact RASMC suggest that Nox4 depletion does not affect Nox1 activity, but reduces Nox4 expression and H_2O_2 production. However, it is possible that other sources of ROS such as mitochondria and xanthine oxidase may contribute to the production of cellular $O_2^{\cdot-}$ and H_2O_2. Therefore, we analyzed directly the activity of NADPH oxidases by $O_2^{\cdot-}$ and H_2O_2 production in membrane fractions isolated from RASMCs treated with scrambled or siNox4 RNA (Figure 6C, D). NADPH-dependent $O_2^{\cdot-}$ production was not affected in membrane fractions of Nox4-depleted cells (Figure 6C) either basally or after Ang II treatment. In contrast, NADPH-dependent H_2O_2 production was significantly lower in Nox4-depleted membrane fractions from untreated cells, but AngII had a similar effect in cells treated with scrambled siRNA or siNox4 RNA (Figure 6D). Interestingly, the activity of NADPH oxidases measured in the membrane fractions showed a similar pattern to ROS production in intact RASMCs (Figure 6). These data confirm that Nox4 is responsible for NADPH-dependent basal H_2O_2 production in the membrane fractions, and suggest that Nox4 mainly generates H_2O_2 (Figure 6C, D).

Previously, it was suggested that failure to detect $O_2^{\cdot-}$ production by Nox4 in living cells may be due to localization of Nox4 in a compartment with high SOD activity [46]. Therefore, we tested the effect of the SOD inhibitor DETC on $O_2^{\cdot-}$ detection by DHE and HPLC. Treatment of intact RASMCs with DETC slightly increased $O_2^{\cdot-}$ detection (1.5±0.1 μM and 1.8±0.2 μM, correspondingly). However, $O_2^{\cdot-}$ production in NOX4-depleted cells was not significantly different from control RASMCs in either untreated or DETC-treated cells (1.6±0.1 μM and 2.0±0.2 μM, correspondingly). Furthermore, our experiments in the membrane fractions (no Cu,Zn-SOD activity) showed NOX4-dependent H_2O_2 release. Therefore, our data do not support the hypothesis that the lack of NOX4-dependent $O_2^{\cdot-}$ is due to NOX4 association with SOD.

Analysis $O_2^{\cdot-}$ and H_2O_2 production in Nox1-depleted RASMCs

In order to confirm that Nox1 is responsible for $O_2^{\cdot-}$ production, we inhibited Nox1 expression using the adenovirus that expresses antisense Nox1 (AdASNox1) as described previously [10,16]. Western Blot confirmed inhibition of Nox1 expression in AdASNox1-treated

RASMCs [10]. Measurement of intracellular $O_2^{\cdot-}$ using DHE-HPLC showed that Ang II is not able to stimulate $O_2^{\cdot-}$ production in Nox1-depleted RASMCs (Figure 7A), which is in line with our previous results [10]. Analysis of cellular H_2O_2 with Amplex Red in Nox1-depleted RASMCs showed attenuation of AngII stimulation, but did not reveal a significant effect on basal H_2O_2 production (Figure 7B).

Activity of NADPH oxidases was directly analyzed by measuring NADPH-dependent $O_2^{\cdot-}$ and H_2O_2 production in membrane fractions isolated from RASMCs treated with vector or AdASNox1 (Figure 7C, D). NADPH-dependent $O_2^{\cdot-}$ production was significantly reduced in membrane fractions of unstimulated and AngII-stimulated cells (Figure 7C). Depletion of Nox1 inhibited Ang II-stimulated H_2O_2 release but did not affect basal H_2O_2 production (Figure 7D). Thus, measurement of NADPH-dependent ROS production in the membrane fractions showed significant impairment of $O_2^{\cdot-}$ production both in basal and Ang II-stimulated cells, with minimal effects on basal H_2O_2 release (Figure 7). These data suggest that both basal and Ang II-stimulated $O_2^{\cdot-}$ production from NADPH oxidases are mediated by Nox1.

DISCUSSION

In this work, we studied the contribution of Nox1 and Nox4 to $O_2^{\cdot-}$ and H_2O_2 production in untreated RASMCs and RASMCs treated with AngII. We found that production of $O_2^{\cdot-}$ by NADPH oxidases was several times less than H_2O_2 production. Depletion of Nox4 in RASMCs treated with siNox4 led to diminished H_2O_2 production, but did not affect $O_2^{\cdot-}$ generation. In contrast, depletion of Nox1 in RASMCs treated with AdASNox1 inhibited basal production of $O_2^{\cdot-}$, as well as AngII-stimulated $O_2^{\cdot-}$ and H_2O_2 production. Therefore, our data suggest that Nox4 produces mainly H_2O_2, while Nox1 generates primarily $O_2^{\cdot-}$.

Previously, production of $O_2^{\cdot-}$ in the membrane preparations of RASMCs was demonstrated by spin trapping techniques [28]. However, quantification of $O_2^{\cdot-}$ radicals with spin traps is limited by stability of the superoxide radical adducts [47], and quantitative comparison of $O_2^{\cdot-}$ and H_2O_2 production was not possible. In this work we have described a new and sensitive assay for $O_2^{\cdot-}$ and H_2O_2 in membrane fractions using ESR spectroscopy with cyclic hydroxylamine CPH (Figure 1, 2) to quantitatively measure the amount of $O_2^{\cdot-}$ and H_2O_2 produced by NADPH oxidases. We found that production of H_2O_2 exceeds $O_2^{\cdot-}$ formation (Figure 2). Interestingly, stimulation of RASMCs with AngII strongly increases $O_2^{\cdot-}$ production, but only slightly raises H_2O_2 formation. Nox4 depletion decreases basal H_2O_2 production, but does not affect $O_2^{\cdot-}$ formation and Ang II-stimulated H_2O_2 production (Figure 5, 6). Meanwhile, Nox1 depletion in AdASNox1- treated cells abolishes basal and AngII-stimulated $O_2^{\cdot-}$ production in the membrane fractions (Figure 7). This analysis of NADPH oxidases activity supports the notion that basal production of H_2O_2 is due to Nox4 activity, while Nox1 is responsible for the most of the basal and Ang II-stimulated $O_2^{\cdot-}$ production.

The decrease in $O_2^{\cdot-}$ production after down-regulation of Nox1 has been previously demonstrated both by DHE [10] and lucigenin [48]. However, lucigenin does not measure the exact amount of superoxide produced. Furthermore, the effect of Nox1 or Nox4 down-regulation on H_2O_2 production has not been investigated due to interference with intracellular SOD. In this work we used a state-of-the-art ESR technique for H_2O_2 detection in membrane fractions, which lack cytosolic Cu,Zn-SOD. Moreover, we measured both cellular $O_2^{\cdot-}$ (DHE) and extracellular H_2O_2 (Amplex Red) in Nox1 and Nox4 depleted cells, which demonstrated distinct regulations of $O_2^{\cdot-}$ and H_2O_2 production.

It is important to note that $O_2^{\cdot-}$ production in intact cells was measured by dihydroethidium, which has higher rate constant of reaction with $O_2^{\cdot-}$ compared to CPH (2×10^6 $M^{-1}s^{-1}$ vs 3.2×10^3 $M^{-1}s^{-1}$) [36,42]. Furthermore, the reaction of $O_2^{\cdot-}$ with dihydroethidium was followed

by accumulation of superoxide specific product 2-hydroxyethidium, while oxidation of CPH is not superoxide specific. Thus, $O_2^{\cdot-}$ detection by CPH should be used in cell-free systems or cellular fractions where detection of superoxide can be confirmed by inhibition of the ESR signal with superoxide dismutase.

This work represents a first attempt to investigate specific ROS produced by Nox1 and Nox4. Although CPH-based techniques offer a unique ability to measure $O_2^{\cdot-}$ and H_2O_2 in membrane fractions, there are a number of limitations to absolute quantitation of ROS, including limited reactivity with $O_2^{\cdot-}$ and potential contamination of the membrane fractions with cellular antioxidants. Although we have made a concerted effort to maximize the efficiency of ROS detection by ESR (Figure 2) and to exclude contamination by thorough centrifugation and control tests with SOD-inhibitor DETC, we also identified limitations of different assays in quantitative detection of ROS in cells or membrane fractions. For example, we found that Amplex Red cannot be used for H_2O_2 detection in membrane fractions due to the interference with NADPH, while in intact cells, Amplex Red measures only H_2O_2 diffused from cells and, therefore, provides only comparative quantitation of cellular H_2O_2. We have also shown that sensitivity of the cytochrome c assay is not sufficient for $O_2^{\cdot-}$ detection in membrane fractions of the cells used in this study (unpublished observations). Detection of intracellular $O_2^{\cdot-}$ by dihydroethidium is substantially hindered by cellular antioxidants such as cytosolic superoxide dismutase and, therefore, accumulation 2-hydroxyethidium provides only comparative quantitation of cellular $O_2^{\cdot-}$.

Serrander et al. [46] suggested that Nox4 may generate $O_2^{\cdot-}$ within an intracellular compartment that is not accessible to DHE or spin probes. They found that overexpression of Nox4 resulted in a higher signal from nitro blue tetrazolium (NBT), but not DHE or spin probe ACP [46]. However, NBT can be reduced by various flavin proteins, probably including Nox4. Therefore, it is possible that increased NBT reduction in Nox4 overexpressing cells is due to NBT redox cycling [49] in the presence of NADPH. Nox can reduce NBT to NBT radical, which reacts with oxygen to produce superoxide. This artificial reduction of NBT will be inhibited by SOD, and reflect Nox4 expression, but not its activity.

It is important to note that the other assays based on oxidation by superoxide used by Serrander et al. (cell permeable probes DHE and ESR probe ACP) did not detect an increase of superoxide in Nox4 overexpressing cells [46], which was explained by a possible lack of accessibility of the probes to NOX4. In our experiments, we used membrane fractions to overcome this potential limitation. For example, NADPH was able to access Nox4 because ROS production was significantly decreased in the membrane preparations of Nox4-depleted cells (Figure 6). Furthermore, $O_2^{\cdot-}$ detection in membrane fractions did not depend on the reactivity or the concentrations of the probes (CPH, CMH or DHE), which are easily permeable to all possible cellular and lipid compartments including mitochondria [50]. Finally, our experiments with DETC-treated RASMCs did not support the hypothesis that the lack of Nox4-dependent $O_2^{\cdot-}$ is due to NOX4 association with SOD. Taken together, these arguments suggest that the major detectable product of Nox4 is H_2O_2.

It has been reported that Nox4 is responsible for constitutive production of H_2O_2 [11], but whether this is derived from dismutation of $O_2^{\cdot-}$ or direct production of H_2O_2 is unclear. It is generally assumed that all Noxes initially produce $O_2^{\cdot-}$, which then dismutates into H_2O_2. However, increased expression of the p22phox subunit increases H_2O_2 production without changing $O_2^{\cdot-}$ generation [34]. This raises the possibility of direct H_2O_2 generation by NADPH oxidases. Previously, production of extracellular H_2O_2 in Nox4 expressing epithelial cells was found to require p22phox, but not the other canonical cytosolic subunits [11]. Based on these observations and the data reported here, we suggest that $O_2^{\cdot-}$ release from the catalytic core of

Nox4 is electrostatically hindered, leading to 2 sequential single-electron reductions by heme, thus favoring H_2O_2 release (Figure 8).

Precedence for direct generation of H_2O_2 without intermediate $O_2^{\cdot-}$ can be found in xanthine oxidase [9], where molybdenum center oxidizes xanthine and transfer electrons to the flavin group, which reduces oxygen by two consecutive electron transfers. Dissociation of the $O_2^{\cdot-}$-xanthine oxidase complex is slow compared with the fast transfer of the second electron to oxygen. This process results in formation of a H_2O_2-xanthine oxidase complex, which rapidly dissociates into H_2O_2 and xanthine oxidase. It has been estimated that 75% of electron flow in xanthine oxidase is involved in two-electron reduction of oxygen. A similar process may occur with Nox4, where the complex of ferric Nox4—$O_2^{\cdot-}$ may be stable enough to transfer the second electron from the flavin to the heme and then to $O_2^{\cdot-}$ producing H_2O_2 (Figure 8). While some $O_2^{\cdot-}$ may escape, explaining the decrease in $O_2^{\cdot-}$ measured after depletion of Nox4 by siRNA [16], the major detectable product from Nox4 is thus H_2O_2. This proposed mechanism of Nox4-mediated H_2O_2 production requires further investigation.

It was previously reported that the phagocytic NADPH oxidase (Nox2) rapidly produces primarily $O_2^{\cdot-}$ [25], which is then dismutated into H_2O_2. Interestingly, the phagocytic NADPH oxidase is hundreds of times more efficient in $O_2^{\cdot-}$ production than are vascular smooth muscle cells [51]. Thus, it is highly unlikely that dissociation of the Nox2-$O_2^{\cdot-}$ complex is slow, allowing rapid $O_2^{\cdot-}$ release before it receives a second electron from Nox2. A similar mechanism appears to account for $O_2^{\cdot-}$ production by Nox1. Once the ferrous Nox1 heme reduces oxygen, this complex rapidly dissociates into $O_2^{\cdot-}$ and ferric Nox1 (Figure 8).

Expression of Nox4 is thousands of times higher than Nox1 (Figure 4), while inhibition of ROS production in Nox1 or Nox4 depleted cells was comparable (Figure 6 and 7). These data suggest that the catalytic activity of Nox4 is much lower than Nox1, which may be associated with slow dissociation of Nox4-$O_2^{\cdot-}$ complex, allowing a second electron transfer to produce H_2O_2. The differences in catalytic activities of Nox1 and Nox4 can be explained by the lack of Nox4 activation by p47phox and Rac1 [11]. Nox4 has a low, but constitutive activity, while Nox1 has low expression, but very high catalytic activity.

It has been previously shown that under normal physiological conditions Nox4 is required for expression of smooth muscle myosin heavy chain, smooth muscle α-actin, and calponin, and is essential for the maintenance of stress fibers in vascular smooth muscle cells [16]. Recently, Nox4 has been implicated in the TGF-beta1-induced conversion of fibroblasts to myofibroblasts by regulating Smad 2/3 activation [19]. Interestingly, depletion of Nox4 reduced angiogenic responses as assessed by the tube formation and wound healing assays, in both human microvascular and umbilical vein endothelial cells, while overexpression of Nox4 enhanced the angiogenic responses in endothelial cells. These effects were mimicked by exogenous H_2O_2 and blocked by H_2O_2 scavenger ebselen [52]. Thus, production of H_2O_2 by Nox4 is important both in physiological and pathological conditions.

Nox4 is constitutively expressed at high levels in a variety of vascular cells: fibroblasts, endothelial and smooth muscle cells. Thus, Nox4 is constantly involved in ROS production and may be responsible for physiological signaling because H_2O_2 can regulate cellular redox status without stimulating oxidative stress. In contrast, production of $O_2^{\cdot-}$ by Nox1 has been implicated in the cardiovascular diseases, such as hypertension and hypertrophy [38]. Our data confirm that Nox1 is responsible for AngII-induced $O_2^{\cdot-}$ production (Figure 8), and given the established association of Ang II, ROS and vascular disease, suggest that it is this oxidase that contributes to pathophysiological levels of oxidative stress in these cells.

It is important to note that Nox1 is involved in both $O_2^{\cdot-}$ and H_2O_2 dependent redox regulation. Nox1-derived $O_2^{\cdot-}$ will be distmutated into H_2O_2, which may trigger specific cell signaling.

Indeed, enhanced Nox1 expression stimulates cell proliferation [53] and vascular hypertrophy [38], which are mediated by H_2O_2 [53,54]. Meanwhile, $O_2^{\cdot-}$ production by Nox1 modulates vascular reactivity and inflammatory reactions [27].

Our results provide a new insight into cellular H_2O_2 production and its physiological role. It is known that both $O_2^{\cdot-}$ and H_2O_2 serve as second messengers to activate multiple intracellular signaling pathways. We speculate that constitutive expression of Nox4 generates sustained local subcellular H_2O_2. Hydrogen peroxide is a much more stable molecule than $O_2^{\cdot-}$ and can diffuse through several cell layers; therefore, Nox4 may be responsible for maintenance of the tissue H_2O_2 level. The local effect of H_2O_2 mediated redox regulation will then depend on the activity of antioxidants, such as reduced glutathione, glutathione peroxidase, peroxiredoxins and catalase.

Overproduction of H_2O_2 leads to depletion of cellular antioxidants and a change in subcellular H_2O_2 distribution, which may result in activation of abnormal cell signaling, resulting in inflammation and cell apoptosis [55]. It has been shown that H_2O_2 can activate xanthine oxidase, which strongly correlates with the progression of cardiovascular diseases [56]. Furthermore, H_2O_2 may be an early determinant of endothelial dysfunction due to redox stimulation of Nox1 activity resulting in NO inactivation [57]. Of note, most of the clinically used antioxidant interventions do not scavenge H_2O_2. For example, the most frequently used vitamin C and E do not react with H_2O_2. Interestingly, ACE inhibitors and AT1 receptor blockers decrease both NADPH oxidase activity and production of cellular H_2O_2 [58], suggesting that this ability may partially underlie their clinical effectiveness.

In summary, our study clearly showed that depletion of Nox4 in RASMCs treated with siRNA to Nox4 leads to diminished H_2O_2 production, but does not affect $O_2^{\cdot-}$ generation. Depletion of Nox1 in RASMCs inhibits production of $O_2^{\cdot-}$, but not basal H_2O_2, in intact cells and membrane fractions. Using a new state-of-the-art ESR assay for quantitative measurements of both $O_2^{\cdot-}$ and H_2O_2 in the membrane fraction, we found that basal H_2O_2 production exceeds $O_2^{\cdot-}$ generation by 3 to 5 times, while stimulation with AngII causes a 2-fold increase in Nox1-dependent $O_2^{\cdot-}$ production. We conclude that Nox4 produces mainly H_2O_2, while Nox1 generates mostly $O_2^{\cdot-}$. Therefore, Nox4 is responsible for the basal production of H_2O_2, while Nox1 is required for AngII stimulated $O_2^{\cdot-}$ production.

ACKNOWLEDGEMENTS

This work was supported by funding from National Institute of Health grants HL38206, HL058863, PO-1 HL058000, PO-1 HL075209 and American Heart Association SDG 0430201N. We thank Dr David Lambeth for providing the Nox4 antibodies.

LITERATURE

1. Harrison DG. Endothelial function and oxidant stress. Clin Cardiol 1997;20:II-11-7.
2. Griendling KK, Sorescu D, Ushio-Fukai M. NAD(P)H oxidase: role in cardiovascular biology and disease. Circ Res 2000;86:494–501. [PubMed: 10720409]
3. Griendling KK, Sorescu D, Lassegue B, Ushio-Fukai M. Modulation of protein kinase activity and gene expression by reactive oxygen species and their role in vascular physiology and pathophysiology. Arterioscler Thromb Vasc Biol 2000;20:2175–2183. [PubMed: 11031201]
4. Huie RE, Padmaja S. The reaction of NO with superoxide. Free Radic Res Commun 1993;18:195–199. [PubMed: 8396550]
5. Powell CS, Jackson RM. Mitochondrial complex I, aconitase, and succinate dehydrogenase during hypoxia-reoxygenation: modulation of enzyme activities by MnSOD. Am J Physiol Lung Cell Mol Physiol 2003;285:L189–L198. [PubMed: 12665464]

6. Rhee SG, Kang SW, Jeong W, Chang TS, Yang KS, Woo HA. Intracellular messenger function of hydrogen peroxide and its regulation by peroxiredoxins. Curr Opin Cell Biol 2005;17:183–189. [PubMed: 15780595]
7. Jones DP. Redefining oxidative stress. Antioxid Redox Signal 2006;8:1865–1879. [PubMed: 16987039]
8. Buettner GR, Ng CF, Wang M, Rodgers VG, Schafer FQ. A new paradigm: manganese superoxide dismutase influences the production of H2O2 in cells and thereby their biological state. Free Radic Biol Med 2006;41:1338–1350. [PubMed: 17015180]
9. Olson JS, Ballou DP, Palmer G, Massey V. The mechanism of action of xanthine oxidase. J Biol Chem 1974;249:4363–4382. [PubMed: 4367215]
10. Lassegue B, Sorescu D, Szocs K, Yin Q, Akers M, Zhang Y, Grant SL, Lambeth JD, Griendling KK. Novel gp91(phox) homologues in vascular smooth muscle cells : nox1 mediates angiotensin II-induced superoxide formation and redox-sensitive signaling pathways. Circ Res 2001;88:888–894. [PubMed: 11348997]
11. Martyn KD, Frederick LM, von Loehneysen K, Dinauer MC, Knaus UG. Functional analysis of Nox4 reveals unique characteristics compared to other NADPH oxidases. Cell Signal 2006;18:69–82. [PubMed: 15927447]
12. Petry A, Djordjevic T, Weitnauer M, Kietzmann T, Hess J, Gorlach A. NOX2 and NOX4 mediate proliferative response in endothelial cells. Antioxid Redox Signal 2006;8:1473–1484. [PubMed: 16987004]
13. Szocs K, Lassegue B, Sorescu D, Hilenski LL, Valppu L, Couse TL, Wilcox JN, Quinn MT, Lambeth JD, Griendling KK. Upregulation of Nox-based NAD(P)H oxidases in restenosis after carotid injury. Arterioscler Thromb Vasc Biol 2002;22:21–27. [PubMed: 11788456]
14. Hilenski LL, Clempus RE, Quinn MT, Lambeth JD, Griendling KK. Distinct subcellular localizations of Nox1 and Nox4 in vascular smooth muscle cells. Arterioscler Thromb Vasc Biol 2004;24:677–683. [PubMed: 14670934]
15. Suh YA, Arnold RS, Lassegue B, Shi J, Xu X, Sorescu D, Chung AB, Griendling KK, Lambeth JD. Cell transformation by the superoxide-generating oxidase Mox1. Nature 1999;401:79–82. [PubMed: 10485709]
16. Clempus RE, Sorescu D, Dikalova AE, Pounkova L, Jo P, Sorescu GP, Schmidt HH, Lassegue B, Griendling KK. Nox4 is required for maintenance of the differentiated vascular smooth muscle cell phenotype. Arterioscler Thromb Vasc Biol 2007;27:42–48. [PubMed: 17082491]
17. Touyz RM, Yao G, Schiffrin EL. c-Src induces phosphorylation and translocation of p47phox: role in superoxide generation by angiotensin II in human vascular smooth muscle cells. Arterioscler Thromb Vasc Biol 2003;23:981–987. [PubMed: 12663375]
18. Seshiah PN, Weber DS, Rocic P, Valppu L, Taniyama Y, Griendling KK. Angiotensin II stimulation of NAD(P)H oxidase activity: upstream mediators. Circ Res 2002;91:406–413. [PubMed: 12215489]
19. Cucoranu I, Clempus R, Dikalova A, Phelan PJ, Ariyan S, Dikalov S, Sorescu D. NAD(P)H oxidase 4 mediates transforming growth factor-beta1-induced differentiation of cardiac fibroblasts into myofibroblasts. Circ Res 2005;97:900–907. [PubMed: 16179589]
20. Cai H, Harrison DG. Endothelial dysfunction in cardiovascular diseases: the role of oxidant stress. Circ Res 2000;87:840–844. [PubMed: 11073878]
21. Lavoie JL, Sigmund CD. Minireview: overview of the renin-angiotensin system--an endocrine and paracrine system. Endocrinology 2003;144:2179–2183. [PubMed: 12746271]
22. Harrison DG, Cai H, Landmesser U, Griendling KK. Interactions of angiotensin II with NAD(P)H oxidase, oxidant stress and cardiovascular disease. J Renin Angiotensin Aldosterone Syst 2003;4:51–61. [PubMed: 12806586]
23. McNally JS, Davis ME, Giddens DP, Saha A, Hwang J, Dikalov S, Jo H, Harrison DG. Role of xanthine oxidoreductase and NAD(P)H oxidase in endothelial superoxide production in response to oscillatory shear stress. Am J Physiol Heart Circ Physiol 2003;285:H2290–H2297. [PubMed: 12958034]
24. Li WG, Miller FJ Jr, Zhang HJ, Spitz DR, Oberley LW, Weintraub NL. H(2)O(2)-induced O(2) production by a non-phagocytic NAD(P)H oxidase causes oxidant injury. J Biol Chem 2001;276:29251–29256. [PubMed: 11358965]

25. Fujii H, Ichimori K, Hoshiai K, Nakazawa H. Nitric oxide inactivates NADPH oxidase in pig neutrophils by inhibiting its assembling process. J Biol Chem 1997;272:32773–32778. [PubMed: 9407051]
26. Griendling KK, Taubman MB, Akers M, Mendlowitz M, Alexander RW. Characterization of phosphatidylinositol-specific phospholipase C from cultured vascular smooth muscle cells. J Biol Chem 1991;266:15498–15504. [PubMed: 1651335]
27. Sorescu GP, Song H, Tressel SL, Hwang J, Dikalov S, Smith DA, Boyd NL, Platt MO, Lassegue B, Griendling KK, Jo H. Bone morphogenic protein 4 produced in endothelial cells by oscillatory shear stress induces monocyte adhesion by stimulating reactive oxygen species production from a nox1-based NADPH oxidase. Circ Res 2004;95:773–779. [PubMed: 15388638]
28. Sorescu D, Somers MJ, Lassegue B, Grant S, Harrison DG, Griendling KK. Electron spin resonance characterization of the NAD(P)H oxidase in vascular smooth muscle cells. Free Radic Biol Med 2001;30:603–612. [PubMed: 11295358]
29. Hanna IR, Hilenski LL, Dikalova A, Taniyama Y, Dikalov S, Lyle A, Quinn MT, Lassegue B, Griendling KK. Functional association of nox1 with p22phox in vascular smooth muscle cells. Free Radic Biol Med 2004;37:1542–1549. [PubMed: 15477006]
30. Dudley SC Jr, Hoch NE, McCann LA, Honeycutt C, Diamandopoulos L, Fukai T, Harrison DG, Dikalov SI, Langberg J. Atrial fibrillation increases production of superoxide by the left atrium and left atrial appendage: role of the NADPH and xanthine oxidases. Circulation 2005;112:1266–1273. [PubMed: 16129811]
31. Miriyala S, Gongora Nieto MC, Mingone C, Smith D, Dikalov S, Harrison DG, Jo H. Bone morphogenic protein-4 induces hypertension in mice: role of noggin, vascular NADPH oxidases, and impaired vasorelaxation. Circulation 2006;113:2818–2825. [PubMed: 16769910]
32. Rajagopalan S, Kurz S, Munzel T, Tarpey M, Freeman BA, Griendling KK, Harrison DG. Angiotensin II-mediated hypertension in the rat increases vascular superoxide production via membrane NADH/NADPH oxidase activation. Contribution to alterations of vasomotor tone. J Clin Invest 1996;97:1916–1923. [PubMed: 8621776]
33. Fridovich I. Quantitative aspects of the production of superoxide anion radical by milk xanthine oxidase. J Biol Chem 1970;245:4053–4057. [PubMed: 5496991]
34. Khatri JJ, Johnson C, Magid R, Lessner SM, Laude KM, Dikalov SI, Harrison DG, Sung HJ, Rong Y, Galis ZS. Vascular oxidant stress enhances progression and angiogenesis of experimental atheroma. Circulation 2004;109:520–525. [PubMed: 14744973]
35. Mügge A, Elwell JH, Peterson TE, Harrison DG. Release of intact endothelium-derived relaxing factor depends on endothelial superoxide dismutase activity. Am J Physiol 1991;260:219–225.
36. Dikalov S, Griendling KK, Harrison DG. Measurement of reactive oxygen species in cardiovascular studies. Hypertension 2007;49:717–727. [PubMed: 17296874]
37. Mohanty JG, Jaffe JS, Schulman ES, Raible DG. A highly sensitive fluorescent micro-assay of H2O2 release from activated human leukocytes using a dihydroxyphenoxazine derivative. J Immunol Methods 1997;202:133–141. [PubMed: 9107302]
38. Dikalova A, Clempus R, Lassegue B, Cheng G, McCoy J, Dikalov S, San Martin A, Lyle A, Weber DS, Weiss D, Taylor WR, Schmidt HH, Owens GK, Lambeth JD, Griendling KK. Nox1 overexpression potentiates angiotensin II-induced hypertension and vascular smooth muscle hypertrophy in transgenic mice. Circulation 2005;112:2668–2676. [PubMed: 16230485]
39. Wingler K, Wunsch S, Kreutz R, Rothermund L, Paul M, Schmidt HH. Upregulation of the vascular NAD(P)H-oxidase isoforms Nox1 and Nox4 by the renin-angiotensin system in vitro and in vivo. Free Radic Biol Med 2001;31:1456–1464. [PubMed: 11728818]
40. Valgimigli L, Pedulli GF, Paolini M. Measurement of oxidative stress by EPR radical-probe technique. Free Radic Biol Med 2001;31:708–716. [PubMed: 11557308]
41. Matsuo T, Shinzawa H, Togashi H, Aoki M, Sugahara K, Saito K, Saito T, Takahashi T, Yamaguchi I, Aoyama M, Kamada H. Highly sensitive hepatitis B surface antigen detection by measuring stable nitroxide radical formation with ESR spectroscopy. Free Radic Biol Med 1998;25:929–935. [PubMed: 9840738]

42. Zielonka J, Sarna T, Roberts JE, Wishart JF, Kalyanaraman B. Pulse radiolysis and steady-state analyses of the reaction between hydroethidine and superoxide and other oxidants. Arch Biochem Biophys 2006;456:39–47. [PubMed: 17081495]
43. Wardman P. Fluorescent and luminescent probes for measurement of oxidative and nitrosative species in cells and tissues: progress, pitfalls, and prospects. Free Radic Biol Med 2007;43:995–1022. [PubMed: 17761297]
44. Dikalov S, Griendling KK, Harrison DG. Measurement of Reactive Oxygen Species in Cardiovascular Studies. Hypertension 2007;49:1–12. [PubMed: 17145983]
45. Zhao H, Joseph J, Fales HM, Sokoloski EA, Levine RL, Vasquez-Vivar J, Kalyanaraman B. Detection and characterization of the product of hydroethidine and intracellular superoxide by HPLC and limitations of fluorescence. Proc Natl Acad Sci U S A 2005;102:5727–5732. [PubMed: 15824309]
46. Serrander L, Cartier L, Bedard K, Banfi B, Lardy B, Plastre O, Sienkiewicz A, Forro L, Schlegel W, Krause KH. NOX4 activity is determined by mRNA levels and reveals a unique pattern of ROS generation. Biochem J 2007;406:105–114. [PubMed: 17501721]
47. Dikalov SI, Li W, Mehranpour P, Wang SS, Zafari AM. Production of extracellular superoxide by human lymphoblast cell lines: Comparison of electron spin resonance techniques and cytochrome C reduction assay. Biochem Pharmacol 2007;73:972–980. [PubMed: 17222393]
48. Manea A, Manea SA, Gafencu AV, Raicu M, Simionescu M. AP-1-dependent transcriptional regulation of NADPH oxidase in human aortic smooth muscle cells: role of p22phox subunit. Arterioscler Thromb Vasc Biol 2008;28:878–885. [PubMed: 18309110]
49. Vasquez-Vivar J, Martasek P, Hogg N, Karoui H, Masters BS, Pritchard KA Jr, Kalyanaraman B. Electron spin resonance spin-trapping detection of superoxide generated by neuronal nitric oxide synthase. Methods Enzymol 1999;301:169–177. [PubMed: 9919565]
50. Becker LB, vanden Hoek TL, Shao ZH, Li CQ, Schumacker PT. Generation of superoxide in cardiomyocytes during ischemia before reperfusion. Am J Physiol 1999;277:H2240–H2246. [PubMed: 10600842]
51. Lassegue B, Clempus RE. Vascular NAD(P)H oxidases: specific features, expression, and regulation. Am J Physiol Regul Integr Comp Physiol 2003;285:R277–R297. [PubMed: 12855411]
52. Datla SR, Peshavariya H, Dusting GJ, Jiang F. Important Role of Nox4 Type NADPH Oxidase in Angiogenic Responses in Human Microvascular Endothelial Cells In Vitro. Arterioscler Thromb Vasc Biol. 2007
53. Yin CC, Huang KT. H2O2 but not O2- elevated by oxidized LDL enhances human aortic smooth muscle cell proliferation. J Biomed Sci 2007;14:245–254. [PubMed: 17124566]
54. Zhang Y, Griendling KK, Dikalova A, Owens GK, Taylor WR. Vascular hypertrophy in angiotensin II-induced hypertension is mediated by vascular smooth muscle cell-derived H2O2. Hypertension 2005;46:732–737. [PubMed: 16172434]
55. Miyoshi N, Oubrahim H, Chock PB, Stadtman ER. Age-dependent cell death and the role of ATP in hydrogen peroxide-induced apoptosis and necrosis. Proc Natl Acad Sci U S A 2006;103:1727–1731. [PubMed: 16443681]
56. Alderman MH. Serum uric acid as a cardiovascular risk factor for heart disease. Curr Hypertens Rep 2001;3:184–189. [PubMed: 11353567]
57. Boulden BM, Widder JD, Allen JC, Smith DA, Al-Baldawi RN, Harrison DG, Dikalov SI, Jo H, Dudley SC Jr. Early determinants of H2O2-induced endothelial dysfunction. Free Radic Biol Med 2006;41:810–817. [PubMed: 16895801]
58. Zafari AM, Ushio-Fukai M, Akers M, Yin Q, Shah A, Harrison DG, Taylor WR, Griendling KK. Role of NADH/NADPH oxidase-derived H2O2 in angiotensin II-induced vascular hypertrophy. Hypertension 1998;32:488–495. [PubMed: 9740615]

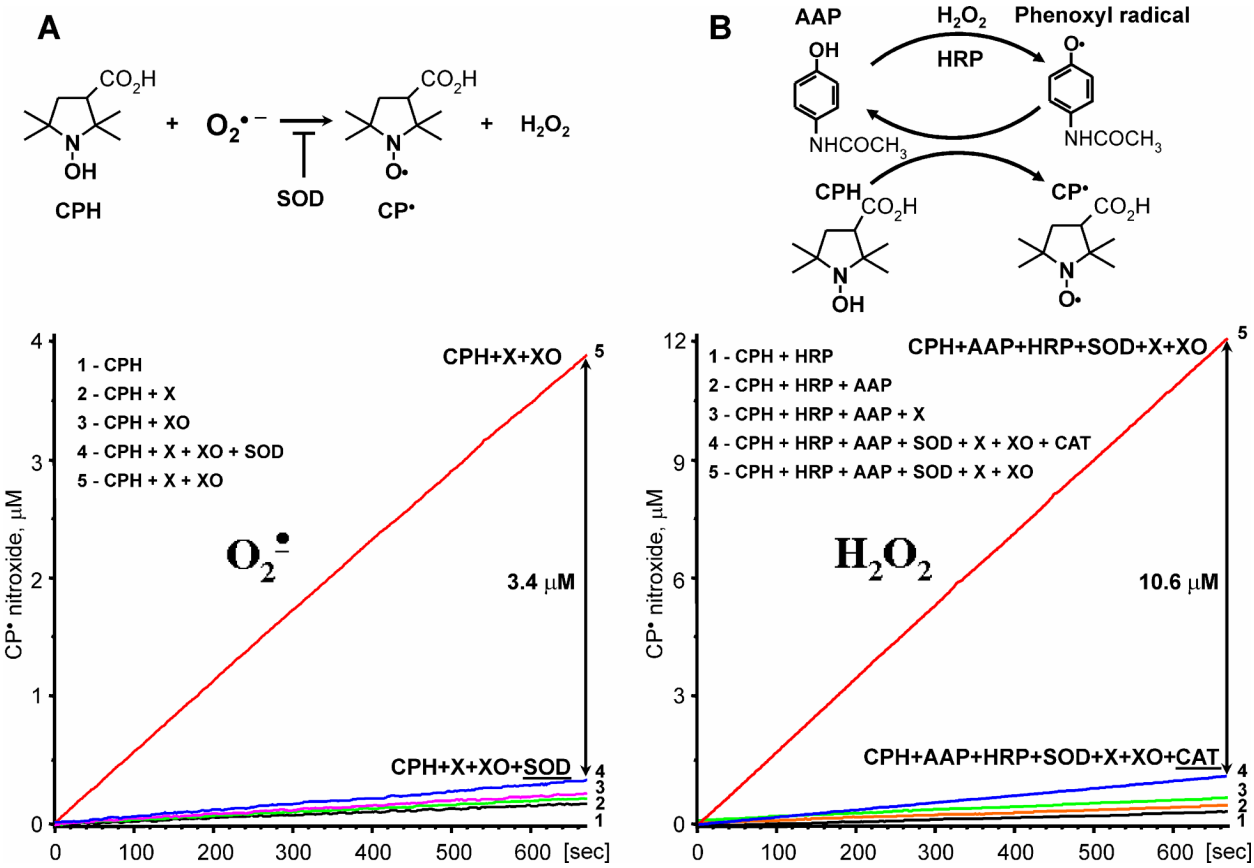

Figure 1.

Quantitative measurements of $O_2^{\cdot-}$ (A) and H_2O_2 (B) in the xanthine oxidase system containing 0.1 mM xanthine and 2 mU/ml xanthine oxidase. Superoxide formation was assayed as SOD-inhibitable formation of 3-carboxy-proxyl (CP), while H_2O_2 was detected by peroxidase-acetamidophenol-mediated co-oxidation of CPH to CP-nitroxide, which was inhibited by catalase (20 μg/ml).

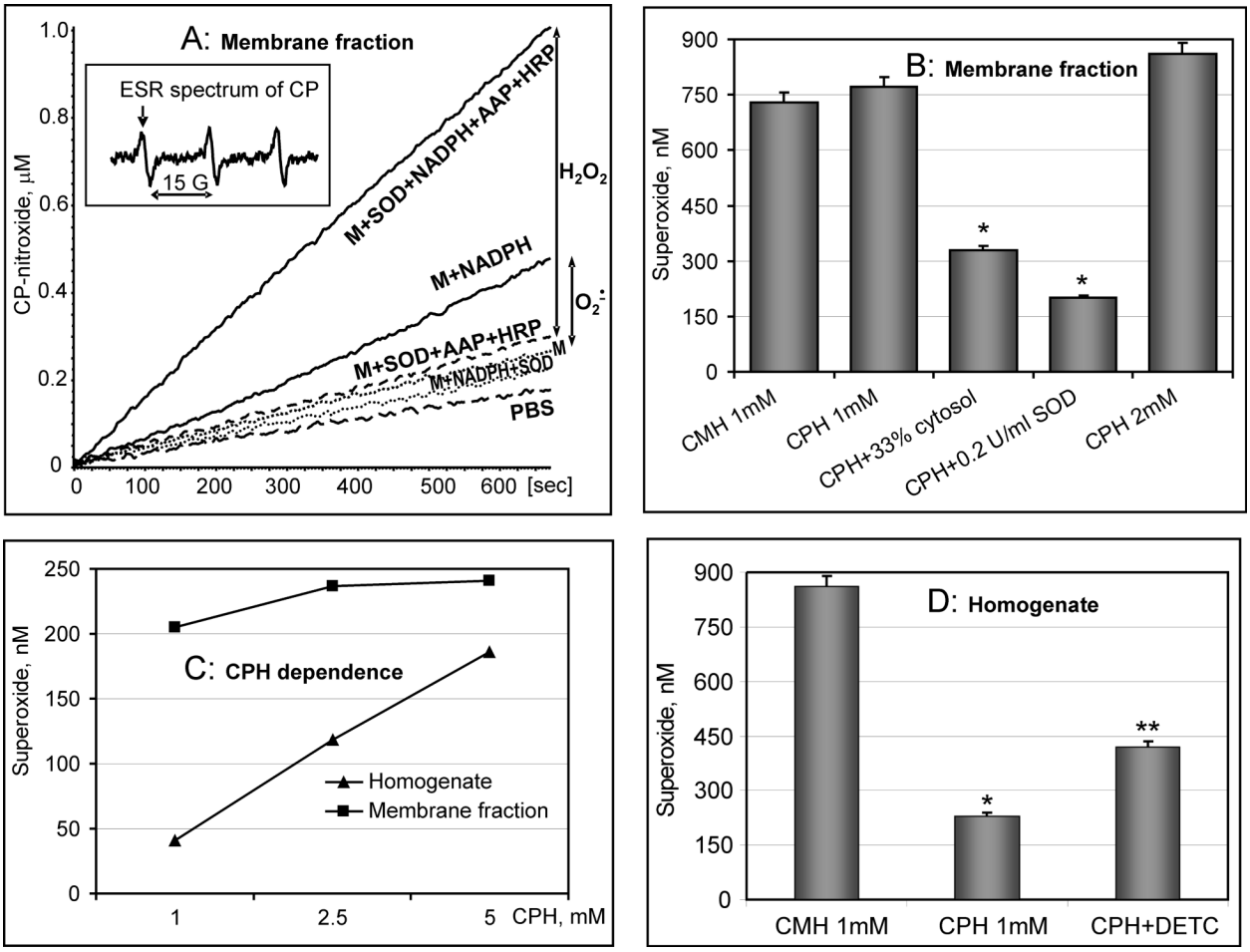

Figure 2.

Analysis of NADPH oxidase activity by measurement of $O_2^{\cdot-}$ and H_2O_2 production in the membrane fraction. (A) Accumulation of 3-carboxyproxyl (CP) in the membrane fraction of RASMCs (0.1mg/ml) followed by an increase in the low-field component of EPR spectrum (insert). The rates of $O_2^{\cdot-}$ and H_2O_2 production were 184 pmol/mg/min and 658 pmol/mg/min, correspondingly. The $O_2^{\cdot-}$ independent H_2O_2 production was 474 pmol/mg/min; (B) Detection of $O_2^{\cdot-}$ in the membrane preparation of RASMCs (0.2 mg/ml) using CMH or CPH. Addition of cytosol inhibited $O_2^{\cdot-}$ detection similar to SOD-supplementation; (C) Measurement of $O_2^{\cdot-}$ production by NADPH oxidase in homogenate and membrane fraction of RASMCs (0.1mg/ml) at various concentrations of CPH; (D) Detection of $O_2^{\cdot-}$ in the homogenate of RASMCs (0.2mg/ml) using CMH, CPH and CPH + SOD-inhibitor DETC.

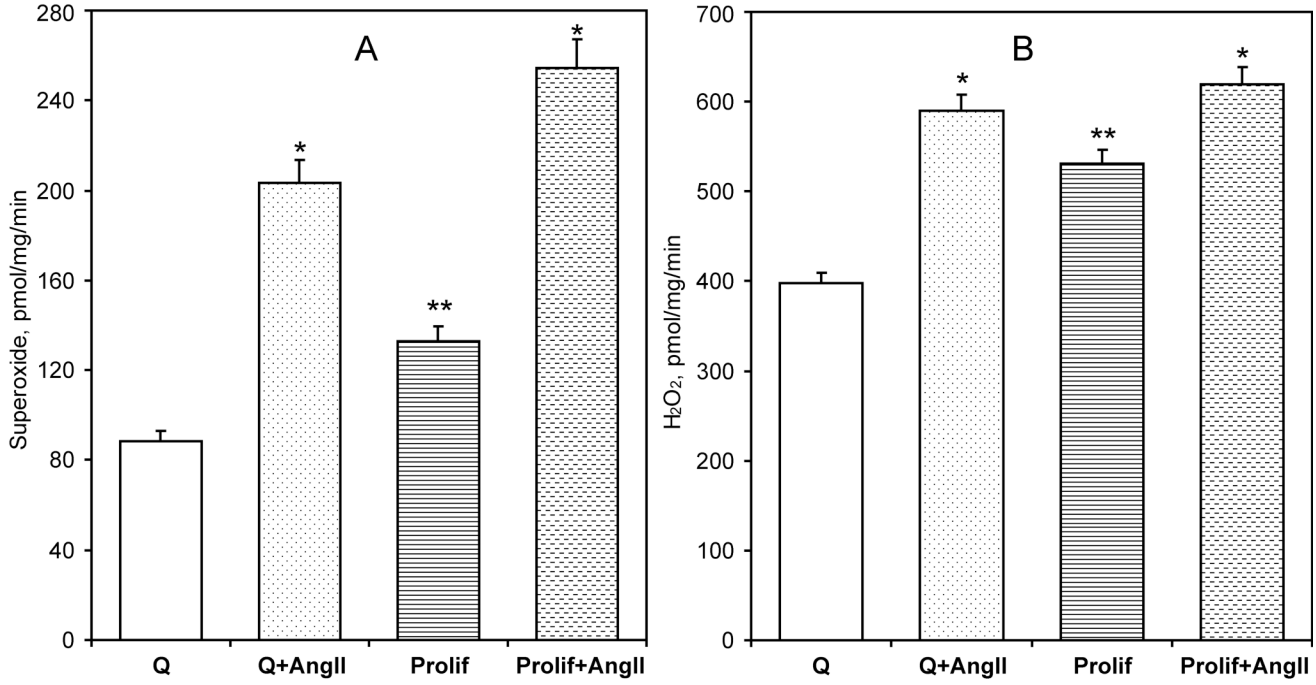

Figure 3.

Stimulation of NADPH oxidase activity in quiescent (Q) or proliferating (Prolif) RASMCs treated with AngII (100 nM) for 4-hours. Activity of NADPH oxidases was analyzed by $O_2^{\cdot-}$ (A) and H_2O_2 (B) production measured in the membrane fraction using ESR spectroscopy as described in the Methods section. Data are from six to eight separate experiments (*P<0.01 Ang II vs unstimulated, **P<0.05 Proliferating vs Quiescent).

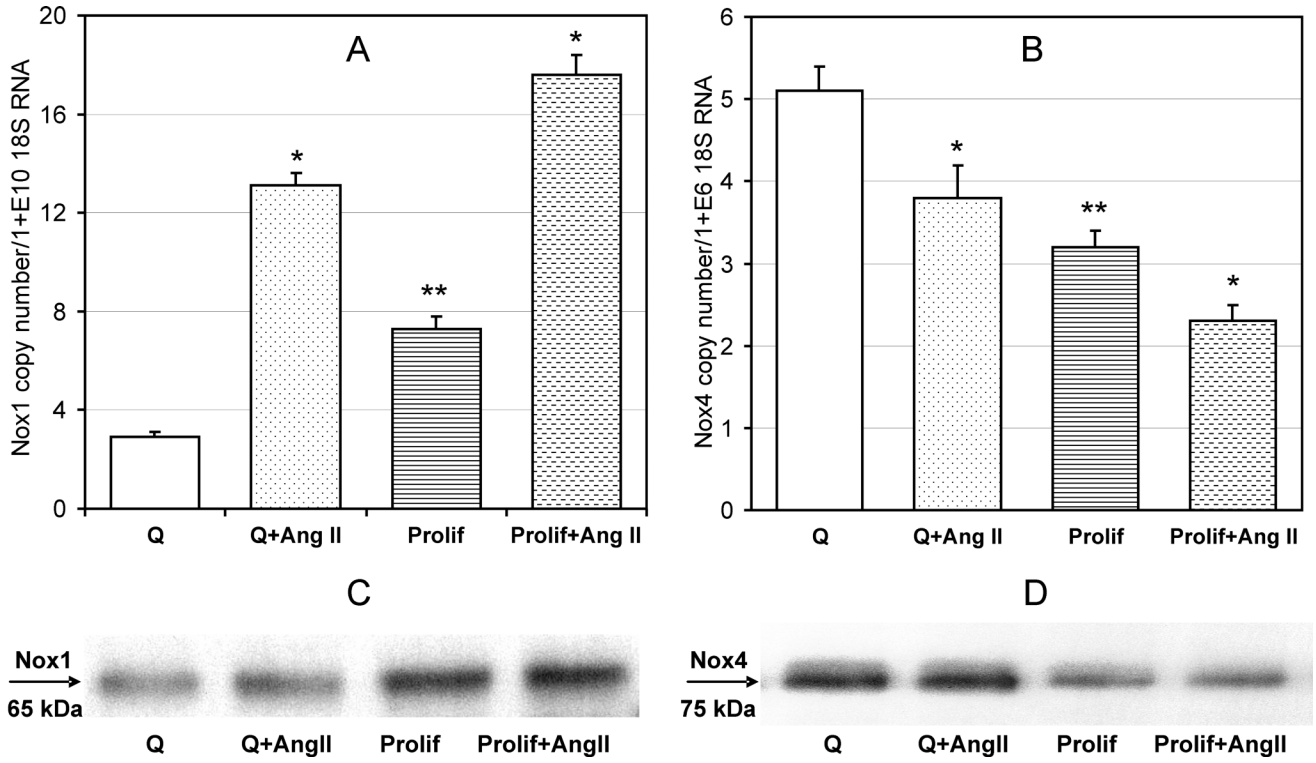

Figure 4.

Expression of Nox1 and Nox4 catalytic subunits in AngII-stimulated (100 nM, 4-hours) quiescent (Q) or proliferating (Prolif) RASMCs measured by real-time PCR (A, B) and Western Blot analysis (C, D). Real-time PCR data are from five separate experiments. Western Blot shows typical expression of Nox1 and Nox4 in quiescent (Q) or proliferating (Prolif) RASMC.

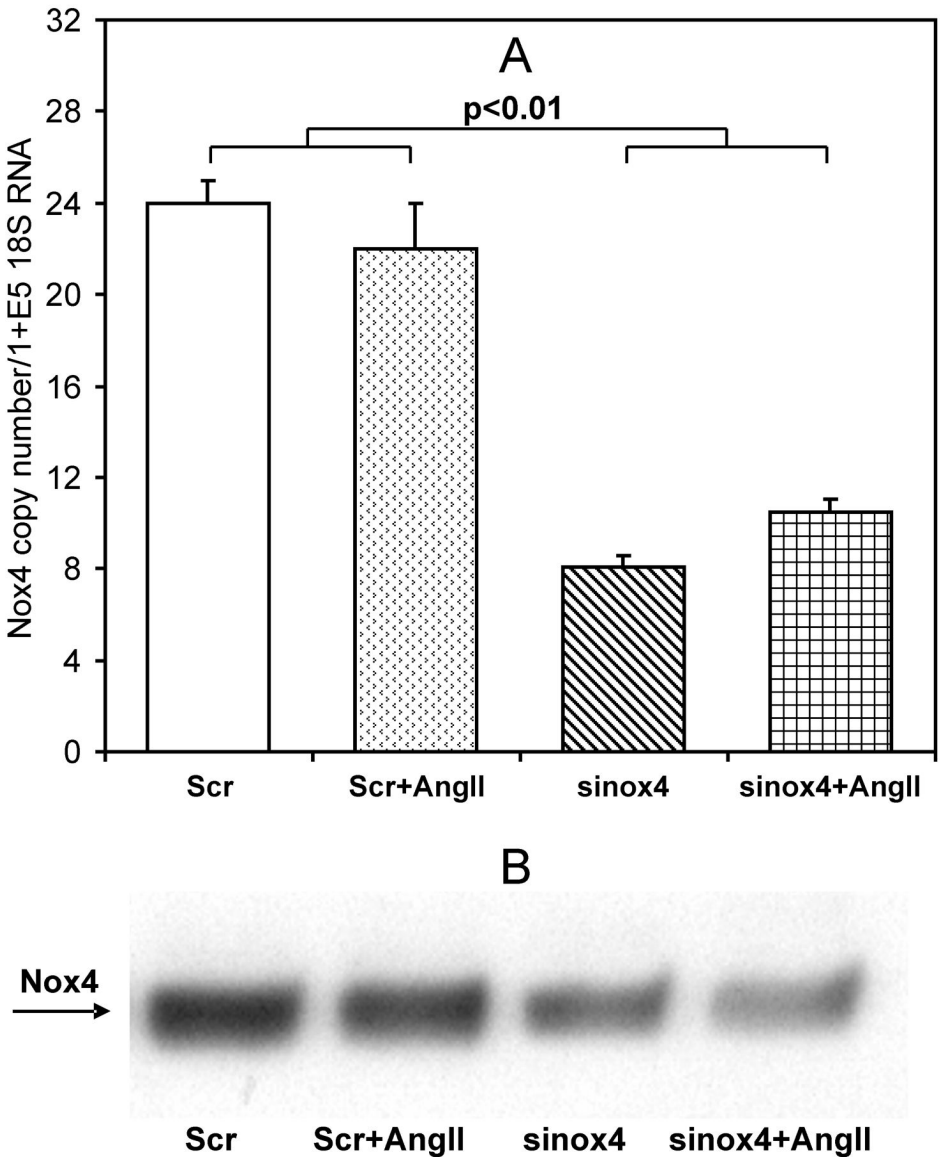

Figure 5.

Expression of Nox4 in siRNA treated RASMCs. RASMCs were treated with scrambled (Scr) or Nox4 siRNA (sinox4) for five days and then stimulated with 100 nM AngII for 4-hours. Expression of Nox4 was measured by real-time PCR (A) and Western Blot analysis (B). Data are average from five separate experiments ± Standard Error. Western Blot shows typical Western blot of Nox4 expression in scrambled or Nox4 siRNA treated RASMCs.

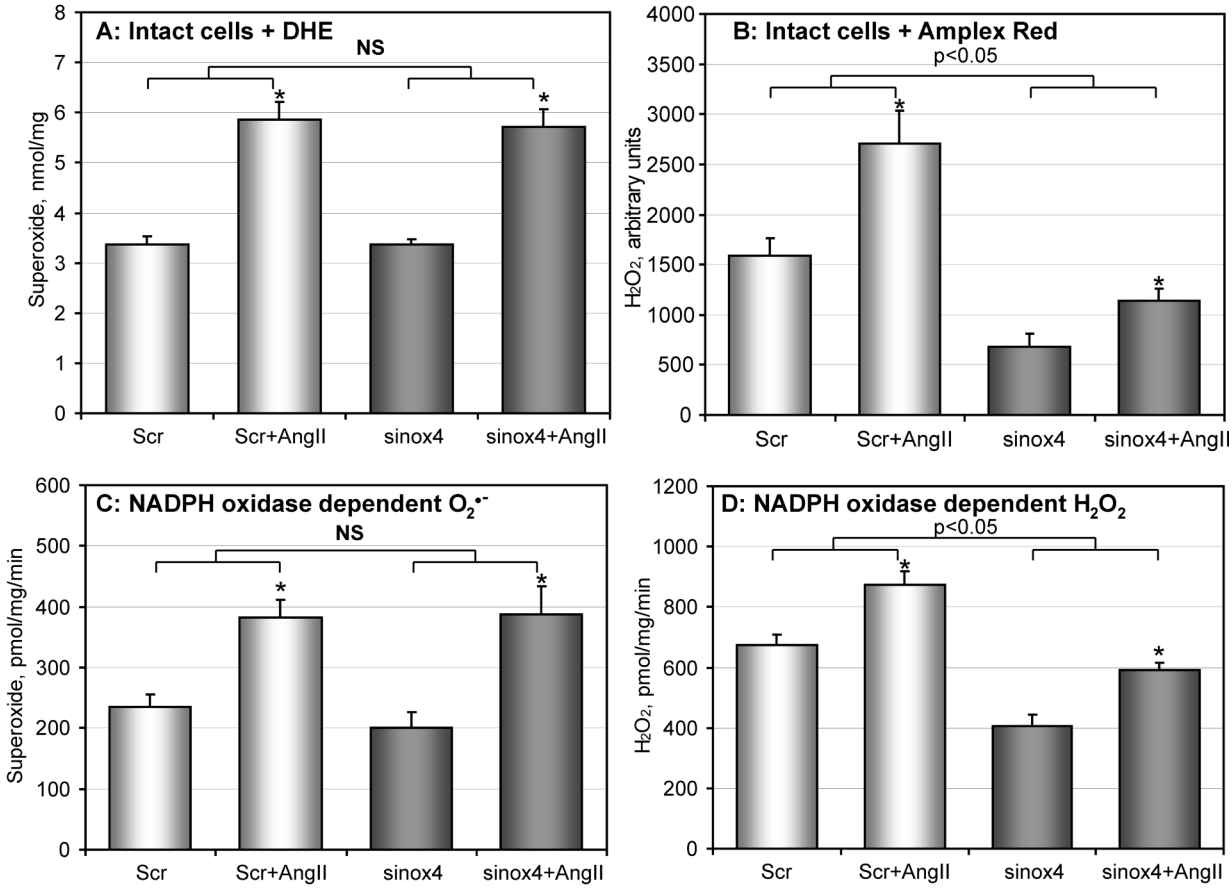

Figure 6.

Analysis of $O_2^{\cdot-}$ and H_2O_2 in Nox4-depleted RASMCs. (A) Production of intracellular $O_2^{\cdot-}$ was measured by DHE/HPLC following accumulation of 2-hydroxyethidium using HPLC as described in Materials and Methods. RASMCs treated with scrambled (Scr) or Nox4 siRNA (sinox4) were stimulated with 100 nM AngII for 4-hours; (B) Cellular H_2O_2 was measured using the fluorescent probe Amplex Red and normalized by cellular protein. RASMCs were stimulated with AngII and incubated with Amplex Red for 2-hours. Accumulation of the fluorescent signal was blocked by supplementation with catalase (20 μg/ml) (not shown). (C) ESR measurements of NADPH oxidase activity in membrane preparations of siRNA-treated RASMC by analysis of NADPH-dependent $O_2^{\cdot-}$ production; (D) Measurements of NADPH oxidase activity in membrane preparations of siRNA-treated RASMC by analysis of NADPH-dependent H_2O_2 production using ESR spectroscopy as described in Methods. Data are from 4 to 6 separate experiments (*P<0.05 AngII vs non-stimulated).

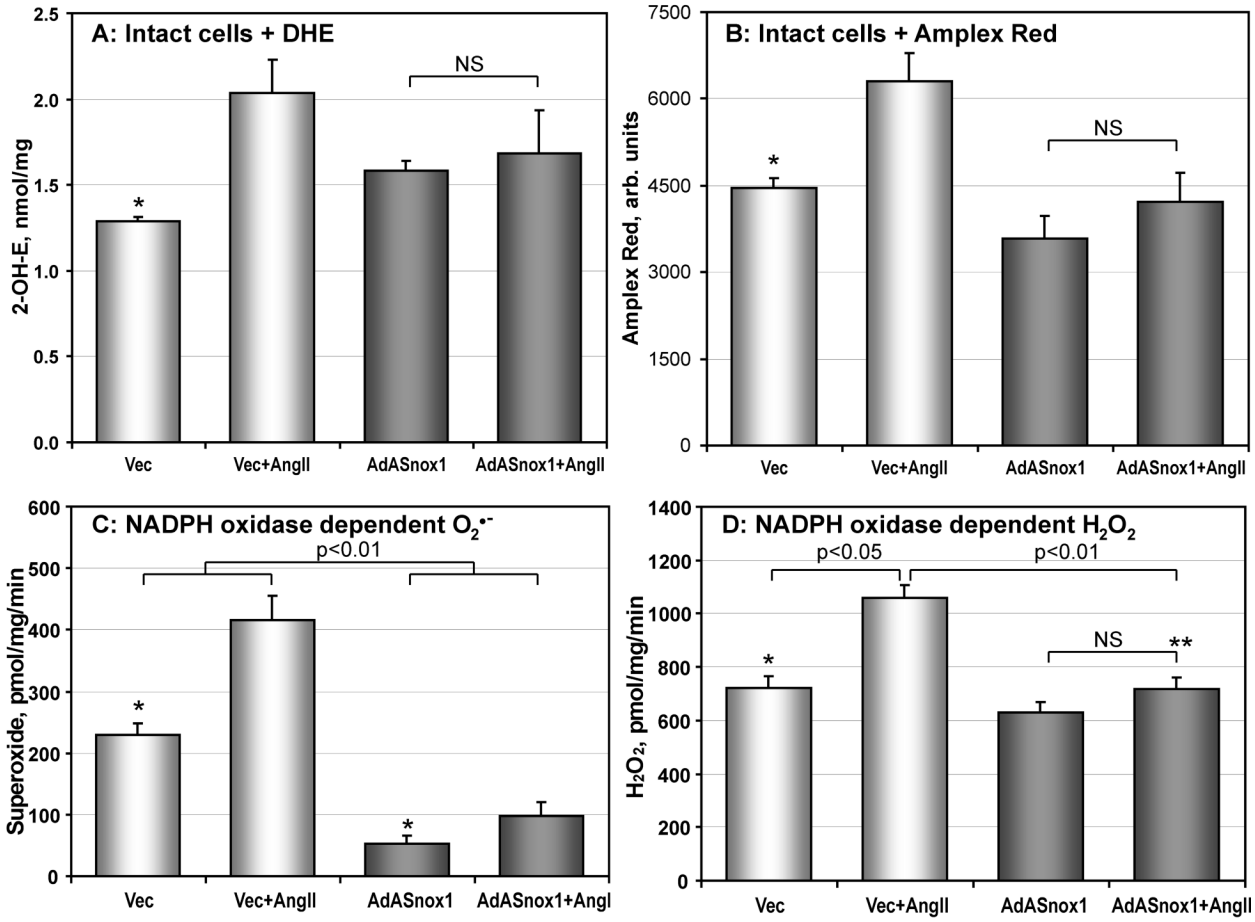

Figure 7.

Analysis of NADPH oxidase activity in Nox1-depleted RASMCs. (A) Production of intracellular $O_2^{\cdot-}$ measured by accumulation of 2-hydroxyethidium using DHE-HPLC as described in Methods. RASMCs treated with vector or AdASNox1 were stimulated with 100 nM AngII for 4-hours; (B) Cellular H_2O_2 was measured using the fluorescent probe Amplex Red and normalized by cellular protein. RASMCs were stimulated with 100 nM AngII and incubated with Amplex Red for 4-hours. Accumulation of fluorescent signal was blocked by supplementation with catalase (20 μg/ml). (C) NADPH oxidase activity measured by $O_2^{\cdot-}$ production in the membrane fraction of RASMCs. (D) (D) NADPH-dependent H_2O_2 production in membrane preparations of RASMCs using ESR spectroscopy as described in Methods. (*P<0.05 vs AngII; **P<0.05 vs Vec+AngII).

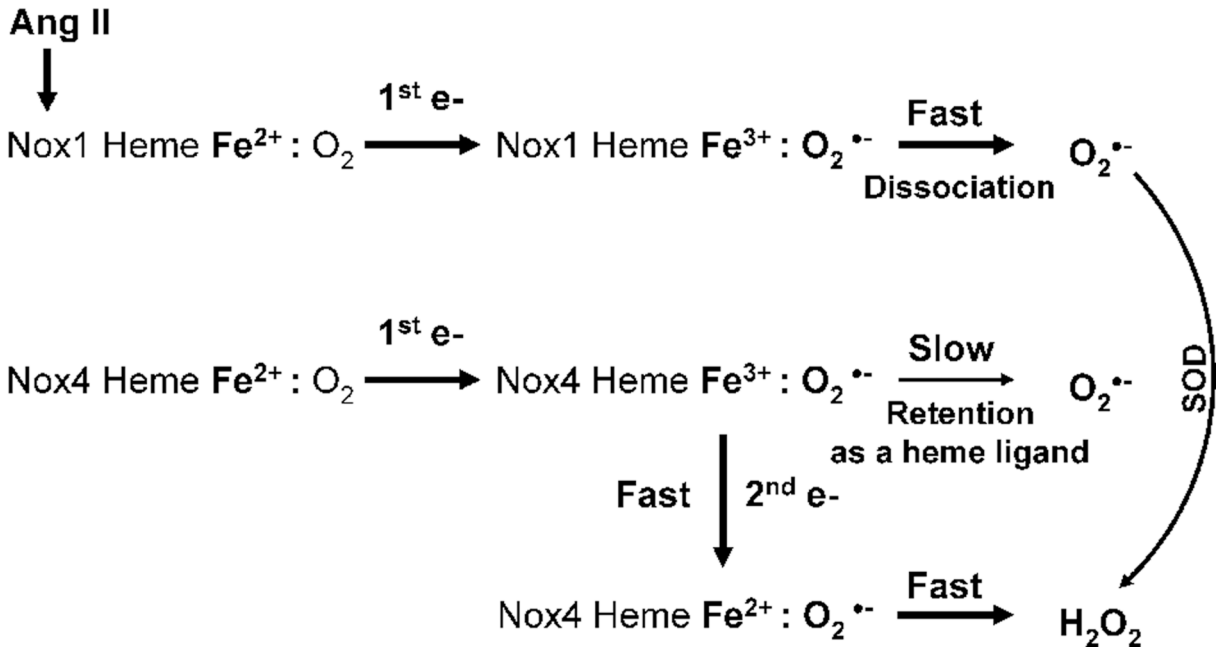

Figure 8.

Potential molecular mechanisms of $O_2^{\cdot-}$ and H_2O_2 production by Nox1 and Nox4. One-electron reduction of oxygen produces a complex of ferric heme and superoxide. The complex of ferric Nox1—$O_2^{\cdot-}$ may rapidly dissociate releasing free $O_2^{\cdot-}$ molecule. Meanwhile, the complex of ferric Nox4—$O_2^{\cdot-}$ may be stable enough to transfer the second electron from the flavin to the heme and then to $O_2^{\cdot-}$, producing H_2O_2.